Accepted Manuscript

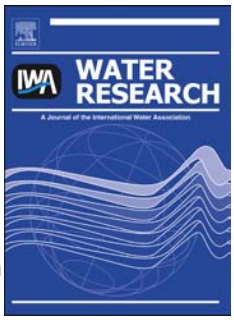

Experimental and Computational investigations of the Interactions between model organic compounds and subsequent membrane fouling

Darli T. Myat, Matthew B. Stewart, Max Mergen, Oliver Zhao, John D. Orbell, Stephen Gray

PII: S0043-1354(13)00712-4

DOI: 10.1016/j.watres.2013.09.020

Reference: WR 10175

To appear in: *Water Research*

Received Date: 20 February 2013

Revised Date: 30 July 2013

Accepted Date: 7 September 2013

Please cite this article as: Myat, D.T., Stewart, M.B., Mergen, M., Zhao, O., Orbell, J.D., Gray, S., Experimental and Computational investigations of the Interactions between model organic compounds and subsequent membrane fouling, *Water Research* (2013), doi: 10.1016/j.watres.2013.09.020.

Experimental and Computational investigations of the Interactions between model organic compounds and subsequent membrane fouling

Darli T. Myat [1], Matthew B. Stewart [1], Max Mergen[2], Oliver Zhao [2], John D. Orbell [1, 3], Stephen Gray[1]

1. *Institute for Sustainability and Innovation (ISI), Victoria University, Melbourne, VIC 8001, Australia,*
2. *Orica Watercare, Melbourne, Vic 3000, Australia,*
3. *College of Engineering and Science, Victoria University, Melbourne, VIC 8001, Australia*

Abstract:

The formation of aggregates of sodium alginate and bovine serum albumin (BSA) (as representative biopolymers) with humic acid were detected by Liquid Chromatography (LC) UV_{254} response in the biopolymer region for mixture solutions. BSA interaction with humic acid showed that aggregation occurred both in the presence and absence of calcium, suggesting that multivalent ions did not play a part in the aggregation process. Similar analyses of the alginate interaction with humic acid also showed a positive interaction, but only in the presence of calcium ions. The fouling characteristics for the BSA-humic acid mixture appeared to be significantly greater than the fouling characteristics of the individual solutions, while for the sodium alginate-humic acid mixture, the fouling rate was similar to that of the sodium alginate alone. The effectiveness of hydraulic backwashing, 10-15% reversibility, was observed for the BSA-humic acid mixture, while the % reversibility was 20-40% for the sodium alginate-humic acid mixture. Increased humic acid and DOC rejection were observed for both BSA-humic acid and sodium alginate-humic acid solutions compared to the individual solutions, indicating that the biopolymer filter cakes were able to

retain humic acids. When compared with BSA-humic acid mixture solution, greater removal of humic acid was observed for alginate-humic mixture, suggesting that sodium alginate may have a greater capacity for associations with humic acid when in the presence of calcium than BSA. Complementary molecular dynamics simulations were designed to provide insights into the specific mechanisms of interaction between BSA and humic acid, as well as between alginate and humic acid. For the BSA-humic acid system; electrostatic, hydrophobic and hydrogen bonding were the dominant types of interactions predicted, whilst divalent ion-mediated bonding was not identified in the simulations, which supported the LC-results. Similarly for the alginate-humic acid system, the interactions predicted were divalent ion-mediated interactions only and this was also supported the LC results. This work suggests that LC-UV_{254} might be used to identify aggregated biopolymers, and that combined with current characterisation techniques, be used to better explain performance variations between water sources.

Key words: organic fouling, microfiltration, liquid chromatography, effluent organic matter, humic acid, biopolymers, molecular dynamics

1. Introduction

Membrane filtration in drinking water treatment and wastewater recovery/reuse involves fouling caused by organic matter (Lee et al., 2004). Many studies of organic fouling have focused on one model NOM foulant for the purpose of understanding the fouling mechanism (Schaefer et al., 2000; Lee and Elimelech, 2006). Fouling studies using natural surface waters reported that hydrophilic (non-humic) components of NOM were more significant foulants

(Carroll et al., 2000; Gray et al., 2007) than the hydrophobic fraction of NOM (Jucker and Clark, 1994), which consists mainly of organic acids and neutrals.

However, in recent times, the focus of studies on organic fouling has shifted from the study of single model foulants to mixtures. The interaction between organic compounds has been identified as an important mechanism in membrane fouling (Jermann et al., 2007; Gray et al., 2008; Gray et al., 2011; Henderson et al., 2011). Jermann et al., (2007) investigated the effect of molecular interactions within and between humics and polysaccharide on UF fouling mechanisms at organic concentration levels relevant for Swiss lakes. A similar study was also conducted by Katsoufidou et al., (2010). Their studies highlighted that when a mixture of two or more fouling species was present in water, interplay between organic foulants (foulant-foulant) as well as foulant-membrane interaction were observed.

Relatively few studies have reported interactions between different organic compounds with respect to fouling by real waters. For example, Gray et al., (2008), in a study of two different surface waters for different membranes, have described the effect of smaller organic acids and proteins on increasing the fouling rate of high molecular weight compounds. Additionally, Kim and Benjamin (2007) have shown that the fouling potential of filtered waters could be similar to that of the original feed water due to the agglomeration of small molecular weight organic compounds that are present in filtered waters. Clearly, the mechanism of organic fouling of low molecular weight compounds is complex. It may involve a range of organic compounds, the predominant foulant may vary with the source of the water and it may be dependent upon the interactions between various components. Therefore, characterization of such organic interactions, including at the molecular level is

important for an understanding of membrane fouling and other water treatment processes, such as organic removal via coagulation or ion exchange.

The aim of this study was to identify possible interactions between organic compounds that are commonly found in natural waters (natural organic matter, NOM) and wastewaters (effluent organic matter, EfOM). Model organic compounds were chosen with structures similar to, or representative of, those considered important in membrane fouling, as well as mixtures of these compounds. More specifically, the compounds used were humic acid, Bovine Serum Albumin (BSA) as an example of a protein and sodium alginate to mimic polysaccharides. Characterizations were performed for solutions in a synthetic background electrolyte of similar composition to that of a municipal wastewater. Liquid chromatography with organic carbon detection (LC-UV_{254}-OCD) and LC coupled with a photo-diode array (PDA) detector were used to probe for interactions in the waters themselves. The ability to identify the presence of interactions between various compounds was thus assessed, and complementary molecular dynamics simulations were used to predict the range of specific interactions that may occur at the molecular level. The computational results were then reconciled with the experimental data. In addition, the fouling response of the specific mixtures with a hydrophobic polypropylene membrane was explored, based on the experimental and theoretical findings observed with the presence of interactions between various organic compounds.

2. Materials and methods

2.1. Organic foulants

Sodium alginate from brown algae (Sigma-Aldrich), bovine serum albumin (BSA, Sigma-Aldrich), and humic acid (HA) (Fluka) were selected as model organic foulants to represent polysaccharides, proteins, and humic acid found in EfOM. Both sodium alginate and BSA (biopolymers) were chosen to represent the high molecular weight compounds present in surface waters and wastewaters, whereas the smaller humic acid was selected to represent the hydrophobic characteristics of organic matter.

2.1.1. Feed solution preparation

Stock solutions (1g/L) were prepared by dissolving each of the foulants in deionized (MilliQ) water. Stock solution of humic acid was adjusted to pH 10 using 5 M sodium hydroxide (NaOH) solution to ensure complete dissolution of the foulants. While raising the pH improved dissolution of the humic acid, a small UV_{254} biopolymer peak was still detected for humic acid solution indicating some residual agglomeration within the humic acid solution.

Model foulant solutions for organic characterization experiments were prepared from the stock solution. 100ml of each model foulant solution was prepared by diluting the required amount of each foulant stock solution to typically 25 mg/L. In order to investigate the interactions between specific species, a range of mixtures containing one biopolymer (either BSA or alginate) and humic acid were prepared and analysed via LC-PDA. When determining the extent of interaction between BSA or alginate and humic acid via UV_{254} in the biopolymer region, the residual humic acid peak in this region was subtracted from the peak for the mixture solutions.

The ionic environment for experiments in electrolyte solution consisted of NaCl (0.003 M), $CaCl_2$ (0.001 M), KCl (0.0004 M) and $MgCl_2$ (0.0004 M) prepared in deionised water. The solutions were adjusted to pH 7-7.5 with 0.01 M hydrochloric acid. The total ionic strength (circa I = 0.77 x 10^{-2} M, 420 mg/L) was confirmed by conductivity measurements. The prepared pH, ionic strength and cation concentrations were chosen because of their similarity to a local secondary effluent wastewater. Table 1 summarises the foulant solutions prepared for organic characterization.

Table 1. Summary of foulant solutions (in electrolyte) prepared for organic characterization

2.2. Water quality analyses and characterisation

Water samples were characterized by pH, conductivity and molecular weight distribution by liquid chromatography (LC). Molecular weight distributions were determined by LC using a photodiode array, (PDA) detector (Method A) as described by Myat et al., 2012, and with LC coupled with UV_{254} (UVD) and organic carbon detector (OCD) (Method B). Analysis by Method B (DOC-Labor) was carried out by the University of New South Wales. This technique was used to confirm the MW of the alginate used in this investigation, as well as providing an analysis of the organic compounds based on molecular weight range and dissolved organic carbon (DOC).

2.3. Membrane filtration

Membrane fouling experiments were undertaken using a single hollow fibre membrane filtration apparatus to examine the fouling rate of feed waters. Feed waters were either specific species or a mixture containing one biopolymer (either BSA or alginate) and humic

149 acid . The hydrophobic membrane material was polypropylene with a nominal pore size of
150 0.2 μm, an outer diameter of 0.50 mm and an inner diameter of 0.25 mm. Tran et al., (2006)
151 has previously determined the contact angle of this membrane material with a Cahn Dynamic
152 Contact Angle Analyser, and it was reported to be 160˚. Single hollow fibre membranes were
153 used for filtration using the method described by Myat et al, 2012. This involved confirming
154 that the clean water permeability of each membrane was within a pre-defined range to ensure
155 individual membranes had similar filtration characteristics, operating the filtration at a
156 constant flux of 50 $kg.m^{-2}.h^{-1}$ and backwashing the membrane every 30 minutes of filtration
157 time.
158
159 The transmembrane pressure (TMP) was recorded with time and the unified membrane
160 fouling index (UMFI) method developed by Huang et al., 2008 and Nguyen et al., 2011 was
161 used to assess membrane performance at constant flux. Fouling indices were calculated using
162 long term filtration data that incorporates backwashing, and from data between filtration and
163 backwash cycles to assess the effectiveness of hydraulic backwashing. The fouling indices
164 were based on a resistance-in-series model (Nguyen et al., 2011). Detailed procedures on
165 analysis or equation derivations can be found in Nguyen et al., 2011. Equation 1 describes the
166 calculation of specific flux or permeability ($kgm^{-2}h^{-1}bar^{-1}$) in which the resistance due to
167 fouling increases linearly with the volume or mass of permeate (V) produced (Nguyen et al.,
168 2011). Membrane performance can be normalized by dividing J by ΔP at any specific mass
169 by the initial or clean membrane condition as shown in equation (2).
170

171 $$J_s = \frac{J}{TMP} = \frac{J}{\Delta P} = \frac{1}{\mu(K_{mem} + k_{total} V)} \quad (1)$$

172

173 $$J'_s = \frac{(\frac{J}{\Delta P})V}{(\frac{J}{\Delta P})_0} = \frac{1}{1+(\frac{k_{total}}{K_{mem}})V} \text{ or } \frac{1}{J'_s} = 1 + (\frac{k_{total}}{K_{mem}})V \quad (2)$$

174

175 where; J_s = specific flux or permeability ($kgm^{-2}h^{-1}bar^{-1}$)

176 J'_s = normalized specific flux

177 V = specific mass (kg/m^2)

178 K_{mem} = resistance of clean membrane

179 k_{total} = total rate constants for resistances

180

181 The inverse of normalized specific flux versus specific mass (kg/m^2) can be used to calculate
182 different fouling indices for process cycles of filtration and backwashing. Hydraulic
183 irreversible fouling index (HIFI) can be calculated by using the starting TMP after each
184 backwash cycle. Increased values of HIFI represent higher rates of irreversible fouling. An
185 assessment of reversibility after each backwash cycle was also obtained from the modified
186 method of van den Brink et al., (2009). The analysis was performed by calculating %
187 reversibility after each backwash cycle by comparing the TMP before backwashing to the
188 TMP following backwashing as described in equation 3, in which 'n' is equal to the number
189 of cycles and R represents the inverse of J's value at the time indicated by the subscript.

190

191 $$\% \text{ Reversibility} = \frac{(R_{final})_{n-1} - (R_{start})_n}{(R_{final})_{n-1}} \times 100\% \quad (3)$$

192

193 2.4. Molecular dynamics (MD) modelling

194

Molecular dynamics simulations were designed in order to provide insights into the specific mechanisms of interaction between the BSA and humic acid, as well as the alginate-humic acid system. The BSA model used was the solved x-ray diffraction crystal structure as archived in the Protein Data Bank database (Majorek et al., 2012). The humic acid model used was the Temple-Northeastern-Birrmingham (TNB) model (Davies et al., 1997). The alginate models used were decamer chains of the three sequences found naturally in algal-sourced alginates. These sequences were poly-α-L-guluronate (GG), poly-β-D-mannuronate (MM) and an alternating guluronate-mannuronate arrangement (GM). The initial construction of the protein-humic acid simulation involved placing six humic acid model molecules around the BSA molecule, at distances further than the non-bonding cut-off (12 Å). This was to ensure that any bonding interactions that occur were not artefacts of the initial simulation state and that they were indicative of actual interactions. The alginate-humic acid simulation was constructed by placing six alginate decamer chains (two of each sequence) approximately 15 Å apart, with six humic acid molecules placed at distances greater than 12 Å away from the alginate molecules as well as each other.

These simulations were constructed using the Visual Molecular Dynamics (VMD) package (Humphrey et al., 1996). These constructs were then solvated, with 15 Å box padding, and ions reflective of the experimental work were randomly added. An initial energy minimization step was used to reduce the energy of water packing and any conflicts via conjugate gradient minimization in the molecular dynamics program-NAMD (Phillips et al., 2005). This minimization involved 10,000 steps for the BSA-TNB system and 20,000 steps for the alginate-TNB system, due to the flexible nature of the alginate chains in use. Simulations were then run under NPT-ensemble conditions, as controlled by a Langevin piston and thermostat in a flexible periodic cell, for 1.5 ns. The electrostatic interactions of

the system were calculated via the Particle mesh Ewald method. All non-bonded interactions were subjected to a switching function at 10Å and cut-off at 12Å which was based on the X-PLOR method. The resulting trajectories were analysed for any intermolecular interactions between the species of interest.

3. Results and Discussion

3.1. Size exclusion chromatography of pure model compounds

Figs. 1a-c plot the UV_{254} and organic carbon detector response of LC (Method B) chromatograms of the model foulant solutions, the quantified compositions of which are given in Table 4 in supporting information (SI). The response of the single model compound solutions shown in Fig 1a-c, show that all the model substances elicit a response from the organic carbon detector (OCD). Also evident from this figure is that the organic acids elicited responses from the UV_{254} detector, whilst the BSA and alginate did not. The humic acid also displayed a small UV_{254} peak in the biopolymer region (see Fig.7 in Supporing Information) indicative of incomplete dissolution of the humic acid.

Fig 1. LC-UVD-OCD (Method B) response of pure compounds representative of organic foulants

When the same solutions were analyzed *via* LC method A, the UV response for sodium alginate was similar to that described above, as no UV absorbance was recorded at the 254 nm wavelength. However, for absorbance between 210-220 nm, sodium alginate showed a slight response, possibly due to the uronic acid nature of the monomers from which alginate

is constructed. BSA absorbed strongly at UV 210-220 nm, which is characteristic of amino groups (Her et al., 2004). Both UV 210 and 254 absorbance for humic acid showed significant values.

Her et al., (2007) has previously used the ratio of UV_{210} to UV_{254} absorbances to calculate a UV absorbance ratio index (URI), to distinguish protein-like substances from other NOM components. This previous work demonstrated that URI values were highest for proteins (13.5 for BSA) and lower for other components such as humic and fulvic acids (1.59 for humic acid, 1.88 for fulvic acid). Two BSA peaks were detected (see Fig.8 in SI), at molecular weights of 10 kDa and 22 kDa, which is not uncommon in commercial samples (de Frutos, 1998). The peak corresponding to a molecular weight of 10 kDa was most likely the monomeric species, eliciting a stronger UV absorbance signal than the 22 kDa peak (likely to be the BSA dimer). Therefore, when calculating the URI value for BSA, the maximum absorbance value at 10 kDa was considered for absorbance at both 254 and 210 nm. URIs calculated for each individual foulant compound (both in electrolyte and aqueous environments) are listed in Table 2.

Table 2. URI values calculated for each individual foulant compound in background electrolyte and aqueous solution

3.2. Specific mixtures by LC (Method A)

Further investigation into the specific nature of these humic acid/BSA or alginate interactions were carried out by preparing specific mixtures containing two components (humic acid and

either alginate or BSA) and analyzing these results by LC (Method A) for any interactions, or lack thereof.

When BSA was present with humic acid and electrolytes, an additional UV_{254} absorbing biopolymer peak (see Fig.9 in SI) was present. The additional peak at a high MW observed in Fig.9 a) and b) (see SI) appeared at a higher molecular weight than the BSA peak. The value of URI at the high molecular weight biopolymer peak (circa >50 kDa; Fig. 9 in SI) was 1.6±0.1. The calculated URI value for BSA was half of the value of the BSA alone (decreased from 22±2 to 11±2, circa 10kDa) due to an increase in the UV_{254} signal, suggesting a positive association between BSA and humic acid. To verify whether the additional peak that appeared at 254 nm was the result of divalent cation mediated association between BSA and humic acid, the solution mixture was prepared at the same concentration in deionized water.

When BSA-humic acid was dissolved in water, the additional UV_{254} absorbing biopolymer peak still appeared (See Fig.10 in SI). The URI value at the high molecular weight biopolymer peak (circa >50 kDa) was 2.2±0.1. The URI value of BSA was depressed by approximately 80% of its original URI value (decreased from 19±1 to 3.7±0.9) suggesting more numerous associations between BSA and humic acid.

Regarding the interactions of BSA and humic acid, the reduction in the URI value of the LC peak attributed to the BSA, when compared to the standard BSA-only result, shows a strong association between the protein and the humic acids. These associations were present in both the electrolyte solution as well as deionized water. This suggests that the specific interactions

involved in this aggregation are not dependent on ions being present to form. Similar analysis was also undertaken for the alginate-humic acid system, and the results reported in Table 3.

Table 3. Comparison of absorbance characteristics for mixtures of compounds in background electrolyte and aqueous solution

.

The alginate-humic acid system showed a positive interaction between the alginate and humic acid in electrolyte solution. With this system, considering that alginate has been shown to not absorb UV light at 254 nm, a peak in the UV_{254} chromatogram can be interpreted as an aggregating interaction between the alginate and the humic acid present. Such an increase in absorption at 254nm was recorded for the high molecular weight peak in the alginate-humic acid electrolyte system. However, no UV_{254} significant increase in peak size was recorded, compared to the humic acid alone peak (see Fig. 7 in SI), for the alginate-humic acid system in aqueous environment. This suggests that the alginate-humic acid interactions are ion mediated.

The behavior of specific mixtures in solution, as described by the above LC results, indicates that the interaction between the low molecular weight organic acids and the larger biopolymer molecules occurs in the synthetic systems in varying amounts. As previously

published studies show (Jermann et al., 2007 and Gray et al., 2011), there can be a change in membrane fouling response, depending on the presence or absence of either a particular component or the interactions between organic compounds. In this study, membrane fouling responses of specific mixtures were tested in order to gain insight into organic fouling of synthetic mixture systems, and to identify if interactions between organic compounds may alter the membrane fouling response.

3.3. Membrane fouling responses by specific mixtures

In order to examine the effect of aggregation on membrane fouling, solutions containing the same mixtures as discussed previously were assessed for their membrane fouling potential in an electrolyte environment. In the following experiments, the mixtures containing two foulants had twice as much organic content as the single foulant solutions, as the same individual compound concentrations were maintained for all experiments.

3.3.1. Fouling studies of BSA, humic acid and BSA-humic acid mixture

Fig. 2 plots the filtered DOC amount (mg/m^2) versus the resistance (inverse of J's). This plot is similar to data plots of specific mass (kg/m^2) versus the inverse of J's (Fig. 3) but allows for the effect of DOC concentration in the mixture to be considered. Fig. 2 clearly shows a greater rate of fouling for the BSA-humic acid mixture compared to the individual organic components. The hydraulic irreversible fouling index (HIFI) results for BSA, humic and BSA-humic mixture are represented in Fig. 3 via the slopes of the data lines.

Fig. 2. Plot of fouling curves of BSA, humic and BSA-humic mixture solutions

Fig. 3. Plot of the inverse J's versus specific mass of BSA, humic and BSA-humic mixture solution (HIFI = slope of lines)

Due to the relatively small size (150 – 5000 Da) of the humic molecules, it is unlikely that humic acid was retained via size exclusion by the 0.2 µm polypropylene membrane. Therefore, humic acid fouls the membrane by adsorption in/onto the membrane. The estimated HIFI value calculated from Fig. 3 was 2.84×10^{-4} m^2/kg after 48 h of filtration time (equivalent to specific mass of 2400 kg/m^2, total backwash cycles of 82). Approximately 25% DOC rejection was observed during 48 h of filtration time, reducing from 7.43 mg/L DOC in the feed to 5.56 mg/L DOC in the permeate. Similarly, the UV_{254} absorbance also decreased from 0.54 to 0.36.

When the BSA-only solution was filtered by a polypropylene membrane, the fouling trend appeared to be similar to humic acid, although the calculated HIFI value of 1.50×10^{-4} m^2/kg was approximately 47% lower than the HIFI value of humic acid (see Fig. 3). Although the HIFI value calculated for BSA solution was lower than for humic acid, it is expected that the adsorption of BSA to hydrophobic membranes could occur. Comparison of DOC in the feed and permeate solutions suggested approximately 5% DOC rejection was achieved for the BSA-only solution.

When the subsequent experiment with the BSA-humic acid mixture was carried out, a change in the fouling trend was observed, with two possible fouling rates evident at different times during the filtration as shown by slope 1 and slope 2 in Fig. 3. The fouling trend of the BSA-humic mixture (mass ratio 1:1) (Fig. 3) showed a slow gradual increase at the beginning of

the filtration time, similar to both the humic acid and BSA only runs. The HIFI value calculated up to 1500 kg/m^2 (slope 1 region as labelled in Fig. 3) of the mixture was 7.29 x10^{-4} m^2/kg, while the slope 2 region had a HIFI value of 2.05x10^{-3} m^2/kg. The HIFI value of the slope 2 region was, therefore, significantly greater than the slope 1 region as well as the rates of fouling for humic acid and BSA alone. The higher HIFI values observed for BSA-humic acid mixture indicate the faster accumulation of an irreversible fouling component compared to the individual BSA or humic acid solutions. Furthermore, the fouling curves shown in Fig. 2 suggest that the faster rate of fouling for the BSA-humic acid mixture was not a result of a greater DOC concentration alone, as the mixture showed a faster rate of fouling when the DOC concentration was considered.

Fig. 4. The % permeability reversibility for humic acid (HA), BSA and BSA-humic acid (BSA+HA) system

The percentage reversible permeability achieved following backwashing of the humic acid, BSA and humic acid-BSA mixture is shown in Fig. 4. BSA showed no recoverable permeability throughout the filtration experiment, while both humic acid and humic acid-BSA mixture displayed a decrease in recoverable permeability initially, while during the latter stages of filtration a slight increase in reversibility was observed. This non-recoverable permeability at the beginning of the process could be due to the adsorption of both humic and BSA to the membrane surface. During the later stages of filtration (i.e., > 40 cycles), filter cake formation could be starting to dominate and therefore, hydraulic backwashing seemed to be more effective. The variation in the % reversibility was maintained between 10-15% after > 40 filtration/backwash cycles. It suggests that the slight increase in reversibility following extended filtration corresponds to filter cake development.

It is also possible that the influence of both humic acid and BSA fouling may further enhance the smaller MW humic acid to be retained in the filter cake via humic acid-BSA interactions. The removal of humic acid from the BSA-humic mixture solution was approximately 5% higher compared to the individual humic acid solution from UV_{254} measurements (see Fig. 11 a) in SI). The overall DOC rejection (%) for the mixture solution was 42% compared to 25% and 5% for the individual humic acid and BSA compounds. Both DOC and UV_{254} data analysis for the permeate solutions is consistent with increased humic acid removal in mixture solutions due to interactions with BSA (protein) compounds. This may cause the increase in HIFI value observed for the BSA-humic acid mixture (Fig. 3) as a result of greater constriction of pores within the filter cake by leading to a more compact structure in the filter cake.

3.3.2. Fouling studies of sodium alginate and sodium alginate-humic acid mixture

Filtration of humic acid, sodium alginate and sodium alginate-humic acid solutions in electrolyte were conducted to ascertain the effect and interactions between humic acid and sodium alginate may have on membrane fouling. Fig. 12 in SI plots the fouling curves of sodium alginate, humic acid and sodium alginate-humic mixture. The HIFI results for sodium alginate, humic and sodium alginate-humic mixture are represented in Fig. 5 via the slopes of the data lines.

Fig. 5. Plot of the inverse of J's versus specific mass of Alginate, humic and Alginate-humic mixture solution (HIFI = slope of lines)

The pressure increase in each filtration cycle was very significant during filtration of the alginate solution. The HIFI value calculated for sodium alginate (see Fig. 5) was 3.43 $x10^{-4}$ m^2/kg in 48 h of filtration time. Approximately 62% DOC rejection was observed, during 48 h filtration time, reducing from 8.73 mg/L DOC in the feed to 3.34 mg/L DOC in the permeate. The fouling trends of sodium alginate-humic acid mixture (mass ratio 1:1) and the sodium alginate solution (Fig. 12 in SI) were similar, but the calculated HIFI value for the mixed solution (5.51 x 10^{-4} m^2/kg) was slightly higher (30% increase) than the sodium alginate value.

From the analysis of the individual filtration cycles for humic acid and sodium alginate, the % reversibility of sodium alginate was maintained between 20-40% over the filtration period. In comparison, the % reversibility for humic acid was only between 5-10% (see Fig. 6). Interestingly, the % reversibility of sodium alginate-humic acid was the similar to that of sodium alginate alone, with the % reversibility being constant at approximately 30% after > 40 filtration/backwash cycles (see Fig. 6).

Fig. 6. The % permeability reversibility for sodium alginate (SA), humic acid (HA) and sodium alginate (SA) + humic acid (HA) systems

Notably, sodium alginate fouling influences the alginate-humic acid mixture filtered with PP membrane, possibly due to pore constriction by complexing with the humic acid, creating an additional cake resistance. This is strengthened by the fact that the removal of humic acid from the mixture solution was approximately 15% higher compared to the individual humic acid compound. Similarly, the overall DOC rejection (%) for the mixture solution was 72% compared to 25% and 62% for the individual humic acid and sodium alginate compounds,

444 indicating that the sodium alginate filter cake may protect the membrane from humic acid.
445 Both DOC and UV_{254} data analysis for the permeate solutions can be found in the Fig. 11 in
446 SI..
447 Similar findings were reported by Jermann et al., (2007), in which they highlighted the
448 alginate cake, or gel in the presence of calcium, was irreversibly adsorbed onto the membrane
449 by formation of an assorted alginate gel with humic acid incorporated in the presence of
450 calcium ions. Although direct comparison cannot be made due to the comparatively high ratio
451 of Ca^{2+}: Na^{+} (1:16) used in their feed solutions, interaction between alginate and humic in the
452 presence of calcium was also demonstrated. The filtration performance of sodium alginate
453 could be strongly affected by the added mono-/divalent ions as proposed by van de Ven et al.,
454 (2008). Katsoufidou et al., (2010) also proposed that the fouling mechanism could vary
455 depending on the ratio of calcium ions and alginate/humic acid concentration in the mixture
456 solution. When compared with the BSA-humic acid solution, a greater rejection of humic
457 acid was observed for the alginate-humic mixture suggesting that alginate in the presence of
458 calcium may associate with humic acid to a greater degree than BSA.
459
460 Both LC results and membrane fouling responses for specific mixtures indicate that the
461 interaction between low molecular weight organic acids and larger biopolymers takes place in
462 the synthetic systems. Such interactions might also be possible in more complex mixtures
463 found in natural waters and wastewater effluents. In order to provide insights into the
464 specific interactions that may be forming in solution, molecular dynamics was employed.
465
466
467
468

3.4. Molecular dynamics (MD) modelling

3.4.1. BSA-humic acid interaction by MD

The hypothesis that the BSA and humic acid were aggregating together in solution, as discussed previously, is supported by the molecular dynamics modeling that was carried out to probe this interaction. The majority of the representative humic acid molecules (TNB model) used in the simulation were observed to interact directly with the BSA model. Regarding the BSA-humic acid system, of the six TNB molecules placed within this simulation, four were identified as binding to the protein within the time frame of the simulation (1.5 ns). Thus, a number of direct interactions between the protein and the TNB molecules were identified.

The most common type of interaction observed throughout this simulation was hydrophobic, involving both aliphatic and aromatic moieties of the humic acid interacting with hydrophobic regions of the protein surface. For such interactions, involving one of the three humic acid aromatic rings, the hydrophobic region on the protein involved a proline residue. More specifically, the aliphatic part of the pyrrolidine ring associated at angles approaching 90° with the plane of the aromatic ring of the humic acid. This interaction shows the characteristics of a ‘t-stack’-like attractive interaction (Börnsen et al., 1986). The average distance of the aliphatic carbon atom to the center of mass of the aromatic ring was calculated to be 3.84 (±0.02) Å, which is close to the experimentally determined average value of 3.7 Å for these types of mixed aliphatic-aromatic π-interactions (Brandl et al., 2001).

493 The next most prevalent interaction type identified in the BSA-humic acid system was
494 hydrogen bonding. The dominant functional groups of the humic acid model that hydrogen
495 bonded with the protein surface were the carbonyl (hydrogen bond acceptor), hydroxyl (both
496 acceptor and donor) and amine (donor) moieties. These groups interacted directly with the
497 side chains of a number of different amino residues, the most common being glycine (via the
498 R-NH_2 group), arginine (R-NH_2), serine (R-OH), lysine (R-NH_3^+), as well as an interaction
499 with a backbone nitrogen atom (R-NH-R').
500
501 Hydrogen bonding was also identified to occur between the BSA and humic models with the
502 TNB model acting as both a hydrogen bond donor as well as an acceptor. These interactions
503 seem quite stable throughout the simulation, with many forming and persisting for several
504 hundred picoseconds of simulation time, until the end of the production run. This is not
505 surprising, given the large number of polar or hydrophilic groups present on the surface of
506 BSA.
507
508
509
510 Another interesting interaction that was identified between the protein and the TNB model
511 was a salt bridge (Fig.13 in SI). Salt bridges may be considered as a special type of hydrogen
512 bond involving a combination of two non-covalent bonds; a neutral R–NH···O-R´ hydrogen
513 bond plus an electrostatic cation-anion interaction (Strop et al., 2000). In this regard, it would
514 be expected that the salt bridge interaction would be stronger than a regular hydrogen bond.
515 From the simulation data, the identified salt bridge was the longest lasting interaction,
516 forming at approximately 0.9 ns into the production run and existing unbroken for the
517 remaining 0.6 ns. This suggests that this interaction was energetically favorable and relatively

strong compared to the hydrogen bonding that was observed, given that no hydrogen bonds lasted this length of simulation time.

Interactions between the protein and humic acid model that were not identified during this simulation, yet were expected, were ion-mediated bonding. Given the number and range of ions in this experiment (i.e. Na^{+}, K^{+}, Ca^{2+} and Mg^{2+}), it was anticipated that an aspect of the interaction would involve ion bridging, especially involving one of the three deprotonated carboxyl groups contained on each of the humic acid models. However, a thorough analysis of the simulation trajectory does not contain any evidence for such cations interacting with the BSA and humic acid model. This initially counterintuitive observation can be reconciled with the experimental results for the BSA and humic acid mixtures in the aqueous environment (i.e. no added ionic strength). As shown previously in Table 4 (see SI), a similar, if not stronger, association was observed between these two species when there were no ions added, compared to the experimental electrolyte environment. This appears to be due to the fact that ions are not directly involved in the interactions of BSA and humic acid. Indeed, a higher ionic strength may actually increase competition between the BSA and surrounding media for the humic acid.

3.4.2. Alginate-humic interaction by MD

For the alginate-humic acid system, only one type of interaction was observed. This involves water-mediated Ca^{2+} bridging between the deprotonated carboxylate moiety of the TNB molecule and a binding pocket on the alginate (Fig.14in SI). The carboxylate group of the TNB model was directly bound to a Ca^{2+} ion, with an average simulated bond distance of

2.14 (±0.10) Å, for the final 0.5 ns of simulation time. This bonded Ca^{2+} ion was observed to interact with three oxygen atoms (two from hydroxyl moieties and one from a deprotonated carboxylate group) of the alginate via water-mediated hydrogen bonding interactions. The distances between the calcium and the alginate oxygen atoms in these interactions were 4.70 (±1.4) Å (hydroxyl #1), 5.05 (±1.29) Å (hydroxyl #2) and 4.75 (±1.76) Å which are typical values for interactions of this type (may range between 4 and 5.5Å (Jalilehyand et al., 2001)).

The type of interactions observed between the components of the BSA-humic acid system are not repeated within the alginate-humic acid simulation. Rather, these interactions are strongly ion-mediated, as the only interactions observed were equivalent to native alginate-alginate bonding mechanisms. This result is not unexpected given that the biopolymer in this simulation, the alginate, is highly negatively charged at a neutral pH with almost complete dissociation of all carboxyl groups. This leads to a relative charge density of one anionic charge per 178 Daltons of mass, compared to BSA which contains one negative charge per 4,149 Daltons. Given that the humic acid model is also anionic at the experimental pH, it would be expected that interactions between these two species would be heavily reliant on the ionic environment, in particular the cationic identity and concentrations. This conclusion is supported by the experimental results, whereby there appeared to be little or no complexation between the alginate and humic acid in deionised water (i.e. the URI value increases slightly) yet there was a positive interaction between the two species in the ionic environment (i.e. the URI decreases). The synthetic wastewater systems investigated here, in conjunction with complementary molecular dynamics simulations, have provided strong evidence that interactions between high molecular weight biopolymers and humic acids can occur, and the

568 experimental membrane fouling results demonstrate that these interactions can effect
569 membrane fouling outcomes.
570
571 3.5. Fouling mechanisms
572
573 Based on the hydraulic backwashing analysis and such interactions evidenced for the organic
574 mixtures by both LC results and molecular dynamics (MD) modelling, overall fouling
575 mechanisms were thus proposed. During filtration of BSA-humic acid mixture, enhanced
576 membrane fouling was observed compared to the individual BSA and humic acid systems
577 similar to the findings reported by Madaeni et al., 2006. Madaeni et al., 2006 reported that
578 lower flux decline and higher humic acid rejection were observed for BSA and humic acid
579 system due to the interactions between these compounds. Indeed, the intermolecular
580 interaction between BSA-humic acid system by molecular dynamics simulations and
581 supported by LC analysis demonstrated a range of interactions – including electrostatic,
582 hydrophobic and hydrogen bonding but no ion-mediated interaction. These dominant types of
583 interactions observed are not as strong as ion-mediated interactions. Therefore, it is possible
584 for rearrangement of the BSA and humic acid molecules to occur at low pressures, resulting
585 in a more compact and hydraulically resistant filter cake. Compression of flocculated
586 suspensions are known to be linked to the strength of the networked structure as measured by
587 the compressive yield strength [de Kretser et al, 2003], with weaker intermolecular
588 interactions leading to reduced strength and easier compressibility. Therefore, it is proposed
589 that the resulting formation of a compact fouling cake layer on the membrane surface during
590 filtration/backwashing cycles for BSA-humic acid mixture occurred as filtration progressed
591 over time. This filter cake was not easily hydraulically backwashed as shown by the %
592 reversibility calculated as shown in Fig. 4. It is not immediately obvious why the fouling

593 layer caused by BSA and humic acid system cannot be easily hydraulic backwashed. Hong et
594 al., (2005) suggested that backwash efficiency is closely linked to the structure of the cake
595 layer formed during particle filtration. Therefore, the lower backwashing efficiency may arise
596 from a more densely packed cake layer that prevents fluid flow. Alternatively, weak
597 interactions between foulant entities might lead to uneven filter cake removal during
598 backwashing of hollow fibres, with localized backwashed regions quickly fouling upon
599 filtration as the filter cake rearranges and stabilises.
600
601 Unlike the BSA and humic acid system, the formation of alginate cake or gel with humic acid
602 incorporated occurred only in the presence of divalent Ca^{2+} ions. This is supported by the
603 increased rejection of humic acids during filtration of sodium alginate and humic acid
604 mixture solution. Interestingly, the experimental results showed that the fouling behaviour of
605 the mixture tends to be close to that of sodium alginate alone, suggesting that humic acid
606 does not greatly affect the alginate filter cake structure. Similarly, the reversibility of fouling
607 by backwashing was similar for both the alginate and alginate-humic acid systems. Le-Clech
608 et al., (2006) showed via direct observation the almost complete removal of fouling layer
609 caused by alginate/bentonite solution from a PVDF membrane by backwashing with
610 permeate solution. A similar finding was also reported by Katsoufidou et al., (2010) in which
611 the authors demonstrated fouling reversibility for a sodium alginate and humic acid mixture
612 was greater than for humic acid filtration for a PES membrane. Addition of humic acid to the
613 alginate-Ca^{2+} system may disturb the resultant network, as humic acid competes with alginate
614 to bind with Ca^{2+}. Such interactions will disrupt alginate packing and potentially lead to
615 reduced cross-linking. This may result in a more open and porous filter cake structure.
616 However, the degree of reversibility upon backwashing for the alginate-Ca^{2+} system was

already high, and further increases in reversibility were detected when humic acid was added. Further analysis is required to confirm this hypothesis..

3.6. Practical Implications

The possibility of interactions between large molecular weight biopolymers and smaller organic acids has been demonstrated with potential implications for membrane operations. Increased fouling was demonstrated for protein-humic acid mixtures, while increased humic acid rejection was demonstrated in the presence of polysaccharides and calcium, and proteins. Currently the performance of coagulation in removing these aggregated structures compared to biopolymer compounds and organic acids in isolation is unknown, but it might be speculated, based on their fouling behaviour with hydrophobic membranes, that they may display behaviour different from the isolated compounds.

However, the detection of biopolymer peaks with LC–UV_{254} is seldom observed for natural waters or wastewater. It might be postulated that this is because of competition between other non-UV absorbing organic species for association with the biopolymers, a lack of available calcium for alginate associations, humic acid associating with smaller molecules or different functional groups on the proteins and polysaccharides than what has been considered (eg. acetylated alginates). Nevertheless, while uncommon, there are examples of biopolymers being detected by LC-UV (Her et al., 2003; Fabris et al., 2007). In the case of Her et al., (2003) a small UV_{254} peak was observed for a secondary effluent, while Fabris et al., (2007) used LC-UV_{260} for characterization of biopolymers from an algal impacted surface water. The potential for these aggregated structures to form may in part explain why predicting

membrane fouling and water quality following coagulation or other pretreatments has been difficult to predict, as the extent of association between species is likely to vary with location and time. Therefore, it may be useful to characterize the biopolymer component of waters using LC-UV (an aggregated component) as well as with LC-Organic Carbon Detector (total biopolymers), to obtain a better understanding of biopolymer behavior in water processes and as a means to better explain the variability between water sources on treatment processes.

4. Conclusion

The characterization of the biopolymer fraction into total and aggregated biopolymer components may be useful in explaining variability between water sources in terms of their treatability by coagulation or other pretreatment processes. The formation of aggregates of alginates or BSA as model biopolymer compounds with humic acid was detected by the UV_{254} response in the biopolymer region for mixture solutions. Interestingly, the interaction of BSA with humic acid occurred both in the presence and absence of calcium, suggesting the divalent ions did not play a part in the aggregation process. Similar analyses of the alginate interaction with humic acid also showed a positive interaction, but only in the presence of calcium ions. When molecular dynamics (MD) modelling was employed to provide insights into these organic interactions in solution, the results were complementary to experimental findings. Molecular dynamic simulations of BSA-humic acid system revealed a number of distinct, direct interactions; electrostatic, hydrophobic and hydrogen bonds were the dominant types of interactions predicted. Similarly for the alginate-humic acid system the modelling study strongly suggested that the interaction was water-mediated Ca^{2+} bridging between the deprotonated carboxylate moiety of the humic acid molecule and a binding pocket on the alginate.

667

668 Such a number of distinct, direct interactions between BSA-humic acid mixture led to
669 enhanced membrane fouling compared to alginate-humic acid mixture (i.e. no enhancement
670 of fouling). The dominant types of interactions observed between BSA-humic acid system
671 are expected not to be as strong as ion-mediated interaction; therefore it is possible for both
672 BSA and humic acid molecules to interact through a variety of modes and to rearrange in the
673 cake layer, allowing the creation of a more compact filter cake morphology. This filter cake
674 was not easily hydraulically backwashed possibly due to lower backwashing efficiency for a
675 more densely packed cake layer or because of uneven backwashing for the hollow fibre
676 system and rapid filter cake rearrangement upon recommencing filtration. Unlike the BSA-
677 humic acid mixture, the interaction between alginate and humic acid was divalent ion-
678 mediated only. Therefore, the formation of alginate cake or gel with humic acid incorporated
679 in the presence of divalent Ca^{2+} ions was possible. However, such alginate-humic-Ca^{2+}
680 fouling layer could easily be disturbed after periodic backwashing with deionized water since
681 the % reversibility for this mixture was maintained throughout the experiment. Additionally,
682 the aggregated alginate-Ca^{2+} binding network could be disrupted by adding the humic acid
683 into the mixture, resulting in a more open, porous structure. However, further analysis is
684 required to confirm this hypothesis.

685

686

687 Acknowledgements

688

689 The authors are grateful to the ARC and Orica for financial support of this project (Australian
690 Postgraduate Award- Industry: LP0989554). The University of New South Wales performed

the LC-OCD analyses. The membranes were generously supplied by Siemens Water Technologies. The authors are thankful for these contributions.

References

Börnsen, K. O., Selze, H. L., Schlag, E. W., 1986. Spectra of isotopically mixed benzene dimers: Details on the interaction of in the vdW bond. Journal of Chemical Physics 85 (4), 1726-1732.

Brandl, M., Weiss, M. S., Jabs, A., Sühnel, J., hilgenfeld, R., 2001. C-H···π-interactions in proteins. Journal of Molecular Biology 307, 357-377.

Carroll, T., King, S., Gray, S. R., Bolto, A. B., Booker, N. A., 2000.The fouling of microfiltration membranes by NOM after coagulation treatment. Water Research 34 (11), 2861-2868.

Davies, G., Fataftah, A., Cherkassky, A., Ghabbour, E. A., Radwan, A., Jensen, S. A., Kolla, S., Paciolla, M. D., Sein, L. T. Jnr., Buermann, W., Balasubramanian, M., Budnick, J., and Xing, B. 1997.Tight metal binding by humic acids and its role in biomineralization, Journal of Chemical Society. Dalton Trans 21, 4047-4060.

de Frutos, M., Cifuentes, A., Diez-Masa, J. C., 1998. Multiple peaks in HPLC of Proteins: Bovine Serum Albumin Eluted in a Reversed-Phase System. Journal of High Resolution Chromatography 21 (1), 18-24.

De Keretser, R.G., Boger, D.V., Scales, P.J., 2003. Compressive Rheology: An overview. Rheology Reviews, 125-165

713 Fan, L., Nguyen, T., Roddick, F. A., Harris, J. L., 2008. Low pressure membrane filtration of
714 secondary effluent in water reuse: Pre-treatment for fouling reduction. Journal of Membrane
715 Science 320 (1-2), 135-142.

716 Fabris, R., Lee, E. K., Chow, C. W. K., Chen, V., Drikas, M., 2007, Pre-treatments to reduce
717 fouling of low pressure micro-filtration (MF) membranes. Journal of Membrane Science 289,
718 231-240

719 Gray, S. R., Ritchie, C. B., Tran, T., Bolto, B. A., 2007.Effect of NOM characteristics and
720 membrane type on microfiltration performance. Water Research 41 (17), 3833-3841.

721 Gray, S. R., Ritchie, C. B., Tran, T., Bolto, B. A., Greenwood, P., Busetti, F., Allpike, B.
722 2008.Effect of membrane character and solution chemistry on microfiltration performance.
723 Water Research 42 (3), 743-753.

724 Gray, S. R., Dow, N., Orbell, J.D., Tran, T., Bolto, B.A., 2011. The significance of
725 interactions between organic compounds on low pressure membrane fouling. Water Science
726 and Technology 64 (3), 632-639.

727 Henderson, R.K., Subhi, N., Antony, A., Khan, S.J., Murphy, K.R., Leslie, G.L., Chen, V.,
728 Stuetz, R.M., Le-Clech, P. 2011. Evaluation of effluent organic matter fouling in
729 ultrafiltration treatment using advanced organic characterisation techniques. Journal of
730 Membrane Science, 382, 50-59.

731 Her, N., Amy, G., Park, H. R., Song, M., 2004. Characterizing algogenic organic matter
732 (AOM) and evaluating associated NF membrane fouling. Water Research 38 (6), 1427-1438.

733 Her, N., Amy, G., Plottu-Pecheux, A., Yoon, Y., 2007. Identification of nanofiltration
734 membrane foulants. Water Research, 41 (17), 3936-3947.

735 Her, N., Amy, G., McKnight, D., Sohn, J., Yoon, Y., 2003. Characterization of DOM as a
736 function of MW by fluorescence EEM and HPLC-SEC using UVA, DOC, and fluorescence
737 detection. Water Research 37 (17), 4295-4303.

738 Hong, S., Krishna, P., Hobbs, C., Kim, D., Cho, J. 2005. Variations in backwash efficiency
739 during colloidal filtration of hollow-fibre microfiltration membranes. Desalination 173. 257-
740 268.

741 Howe, K. J., Clarke, M. M., 2002.Fouling of microfiltration and ultrafiltration membranes by
742 natural waters. Environmental Science and Technology 36 (16), 3571-3576.

743 Humbert, H., Gallard, H., Jacquemet, V., Croue, J.-P., 2007. Combination of coagulation and
744 ion exchange for the reduction of UF fouling properties of a high DOC content surface water.
745 Water Research 41 (17), 3803-3811.

746 Humphrey, W., Dalke, A., Schulten, K., 1996.VMD – Visual Molecular Dynamics. Journal
747 of Molecular Graphics 14 (1), 33-38.

748 Jalilehvand, F., Spångberg, D., Lindqvist-Reis, P., Hermansson, K., Persson, I., Sandström,
749 M., 2001. Hydration of the calcium ion. An EXAFS, large-angle X-ray scattering, and
750 molecular dynamics simulation study. Journal of American Chemical Society 123, 431-441.

751 Jermann, D., Pronk, W., Meylan, S., Boller, M., 2007. Interplay of different NOM fouling
752 mechanisms during ultrafilration for drinking water production. Water Research 41 (8), 1713-
753 1722.

754 Jucker, C., Clark, M. M., 1994.Adsorption of humic substances on hydrophobic ultrafiltation
755 membranes. Journal of Membrane Science 97, 37-52.

Katsoufidou, S. K., Sioutopoulos, C. D., Yiantsios, G. S., Karavelas, J. A., 2010. UF membrane fouling by mixtures of humic acids and sodium alginate: Fouling mechanisms and reversibility. Desalination 264, 220-227.

Kim, J., Shi, W., Yuan, Y., Benjamin, M. M., 2007.A serial filtration investigation of membrane fouling by natural organic matter. Journal of Membrane Science 294 (1-2), 115-126.

Le-Clech, P., Marselina, Y., Stuetz, R., Chen, V. 2006. Fouling visualization of soluble microbial product models in MBRs. Desalination 199, 477-479. Lee, N. H., Amy, G., Croue, J. -P., 2004.Identification and understanding of fouling in low pressure membrane (MF/UF) filtration by natural organic matter (NOM). Water Research 38 (20), 4511-4523.

Madaeni, S. S., Sedeh, N. S., Nobili, d. M. 2006. Ultrafiltration of humic substances in the presence of protein and metal ions. Transport in Porous Media 65, 469-484.

Majorek, K. A., Porebski, P. J., Dayal, A., Zimmerman, M. D., Jablonska, K., Stewart, A. J., Chruszcz, M., Minor. W., 2012.Structural and immunological characterisation of bovine, horse, and rabbit serum albumins. Molecular Immunology 52 (3-4), 174-182.

McGaughey, G. B., Gagné, M., Rappé, A., 1998. K. π-Stacking interactions – Alive and well in proteins. Journal of Biological Chemistry 273 (15), 15458-15463.

Myat, D.T., Mergen, M., Zhao, O., Stewart, M.B., Orbell, J.D., Gray, S., 2012. Characterisation of organic matter in IX and PACl treated wastewater in relation to the fouling of hydrophobic polypropylene membrane. Water Research 46, 5151-5164.

Phillips, J. C., Braun, R., Wang, W., Gumbart, J., Tajkhorshid, E., Villa, E., Chipot, C., Skeel, R. D., Kale, L., Schulten, K., 2005.Scalable molecular dynamics with NAMD. Journal of Computational Chemistry 26 (16), 1781-1802.

779 Shon, K. H., Vigneswaran, V., Kim, S. I., Cho, J., Ngo, H. H. 2004.The effect of pre-
780 treatment to ultrafiltration of biologically treated sewage effluent: a detailed effluent organic
781 matter (EfOM) characterization. Water Research 38 (7), 1933-1939.

782 Strop, P., Mayo, S. L., 2000. Contribution of surface salt bridges to protein stability.
783 Biochemistry 39 (6), 1251-1255.

784 van de Ven, W.J.C., van't Sant, K., Punt, I. G. M., Zwijnenburg, A., Kemperman, A.J.B., van
785 der Meer, W. G. J., Wessling, M. 2008. Hollow fibre dead-end ultrafiltration: Influence of
786 ionic environment on filtration of alginates. Journal of Membrane Science 308 (1-2), 218-
787 229.

788 Ye, Y., Le-Clech, P., Chen, V., Fane, A. G., Jefferson, B. 2005. Fouling mechanism of
789 alginate solutions as model extracellular polymeric substances. Desalination 175 (1), 7-20.

790

Figure Captions

Fig 1. LC-UVD-OCD (Method B) response of pure compounds representative of organic foulants

Fig. 2. Plot of fouling curves of BSA, humic and BSA-humic mixture solutions

Fig. 3. Plot of the inverse J's versus specific mass of BSA, humic and BSA-humic mixture solution (HIFI = slope of lines)

Fig. 4. The % permeability reversibility for humic acid (HA), BSA and BSA-humic acid (BSA+HA) system

Fig. 5. Plot of the inverse of J's versus specific mass of Alginate, humic and Alginate-humic mixture solution (HIFI = slope of lines)

Fig. 6. The % permeability reversibility for sodium alginate (SA), humic acid (HA) and sodium alginate (SA) + humic acid (HA) systems

Table 1

Summary of foulant solutions (in electrolyte) prepared for organic characterization

Model foulant solutions	pH (±0.2)	Conductivity (±5µS/cm)
Sodium alginate	7.6	619
BSA	7.2	620
Humic acid (HA)	7.2	627
BSA + HA	7.0	635
Sodium alginate + HA	7.1	634

Table 2

URI values calculated for each individual foulant compounds in background electrolyte and aqueous solution

Model foulant substance	URI (aqueous)	URI (electrolyte)
Sodium Alginate	-*	-*
BSA	19±1	22±2
Humic acid (HA)	1.3±0.1	1.4±0.1

*UV 254nm absorbance 0, therefore a URI value could not be calculated.

Table 3
Comparison of absorbance characteristics for mixtures of compounds in background electrolyte and aqueous solution

	Aqueous			Electrolyte		
	URI-Humic or Tannic	URI-BSA	URI-biopolymer	URI-Humic or Tannic	URI-BSA	URI-biopolymer
Mixture	5000<MW<150	MW~10kDa	MW>=50 kDa	5000<MW<150	MW~10kDa	MW>=50 kDa
BSA-humic	1.1±0.1	3.7±0.9	2.2±0.1	0.9±0.2	11±2	1.6±0.1
Alg-Humic	1.3±0.1	-		1.4±0.4	-	11.5±0.9

*URI could not be calculated as UV_{254} was zero.

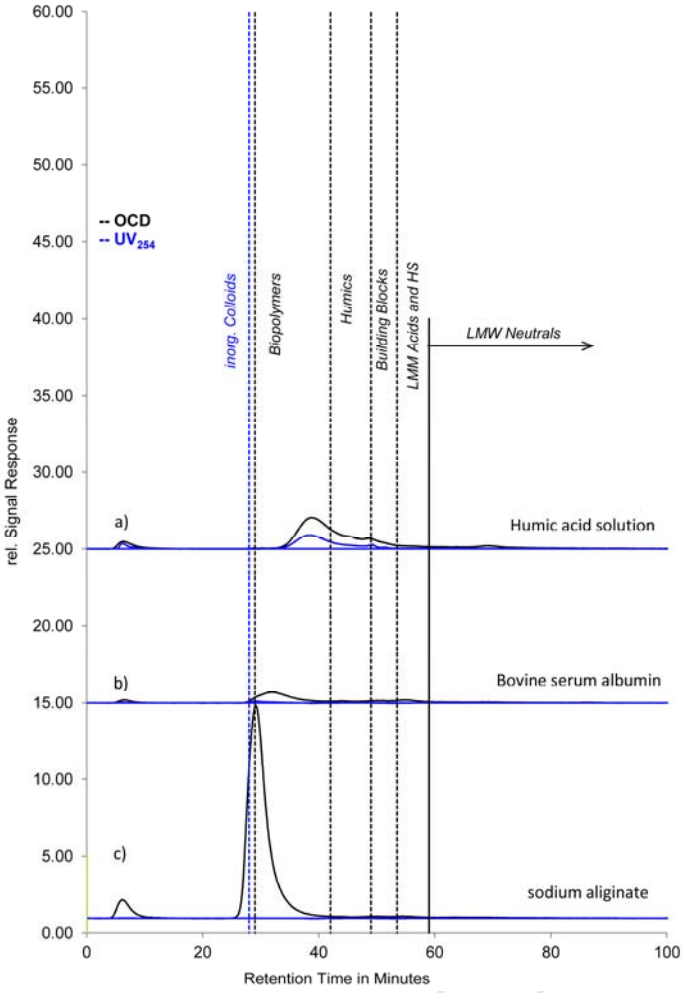

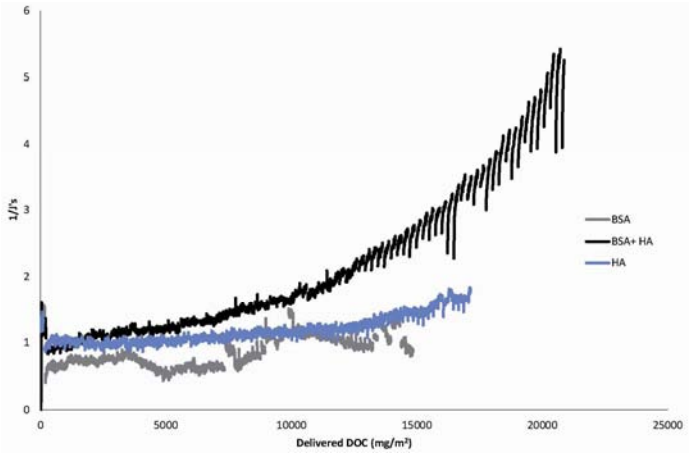

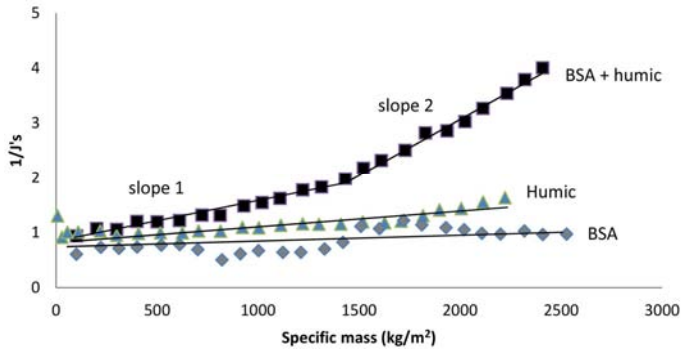

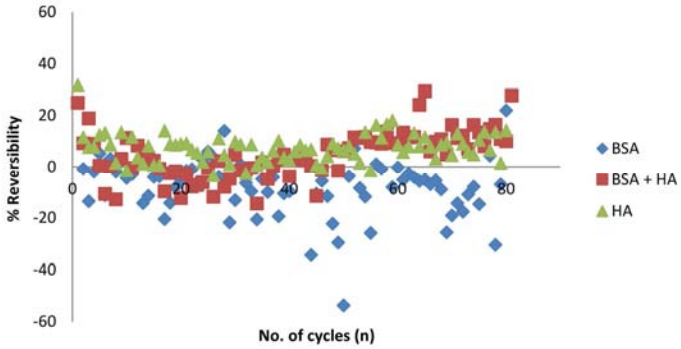

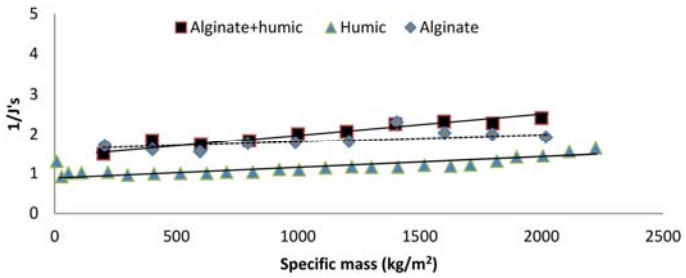

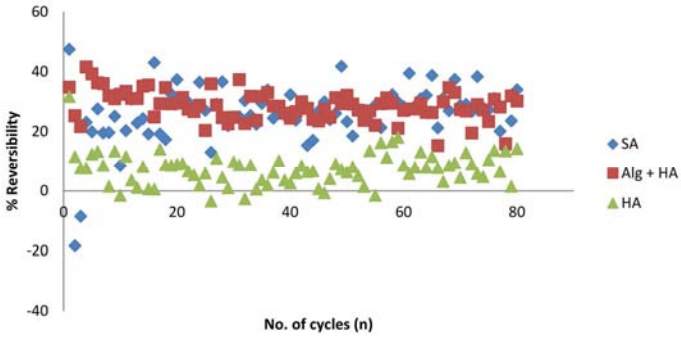

Highlights

- Biopolymers UV254 adsorption indicative of organic acid and biopolymer associations
- Protein-humic acid aggregate due to electrostatic, hydrophobic and hydrogen bonding
- Divalent ion mediated associations between humic acid and polysaccharides
- Protein humic acid associations result in more significant fouling
- Increased rejection of organic acids due to associations with biopolymers

Supplementary Data

Table 4.LC Method B results HA, BSA and Alginate

	Biopolymers	Humic substances	Aromaticity (SUVA – HS)	Building blocks	LMW neutrals	LMW Acids	Inorganic colloids	SUVA
Molecular Weight (Da)	>>20,000	~1,000	~1,000	300-500	<350	<350		
Model substance	ppb-C	ppb-C	L/(mg*m)	ppb-C	ppb-C	ppb-C	m^{-1}	L/(mg*m)
a) HA	12	826	10.16	306	229	3	0.00	8.86
b) BSA	274	63	1.01	78	55	n.q.	1.31	n.q.
c Alginate	2732	n.q.	-	497	57	31	0.04	n.q.

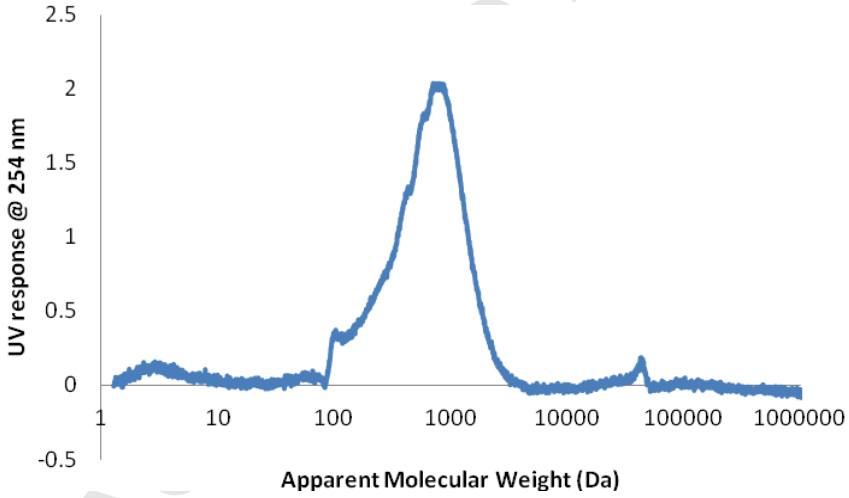

Fig.7. Chromatograms of UV response at 254 nm for humic acid only in deionised solution (Method A)

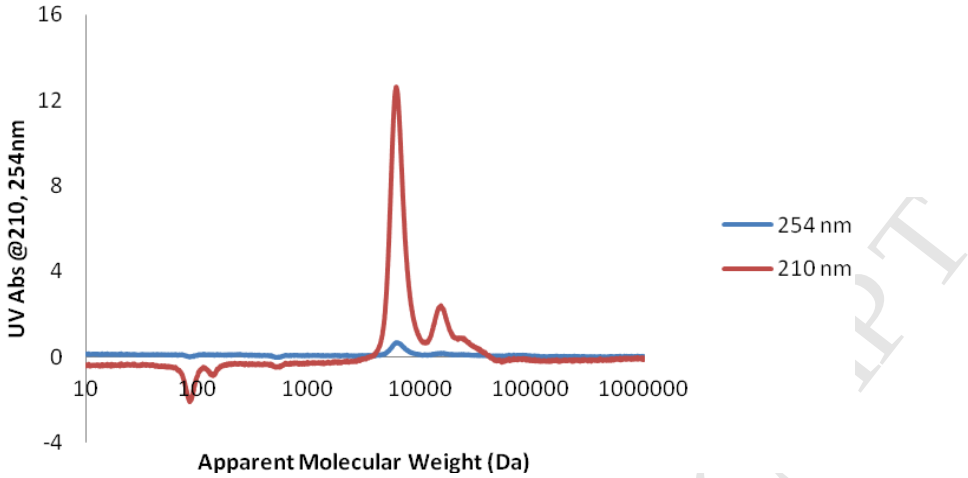

Fig.8. Chromatograms of UV response at 254 nm and 210 nm for BSA only in electrolyte solution (Method A)

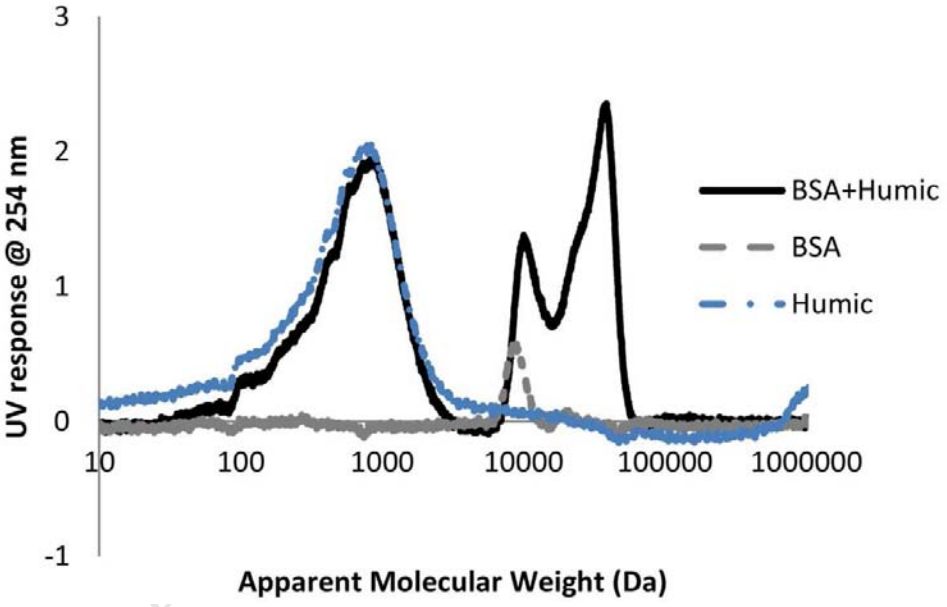

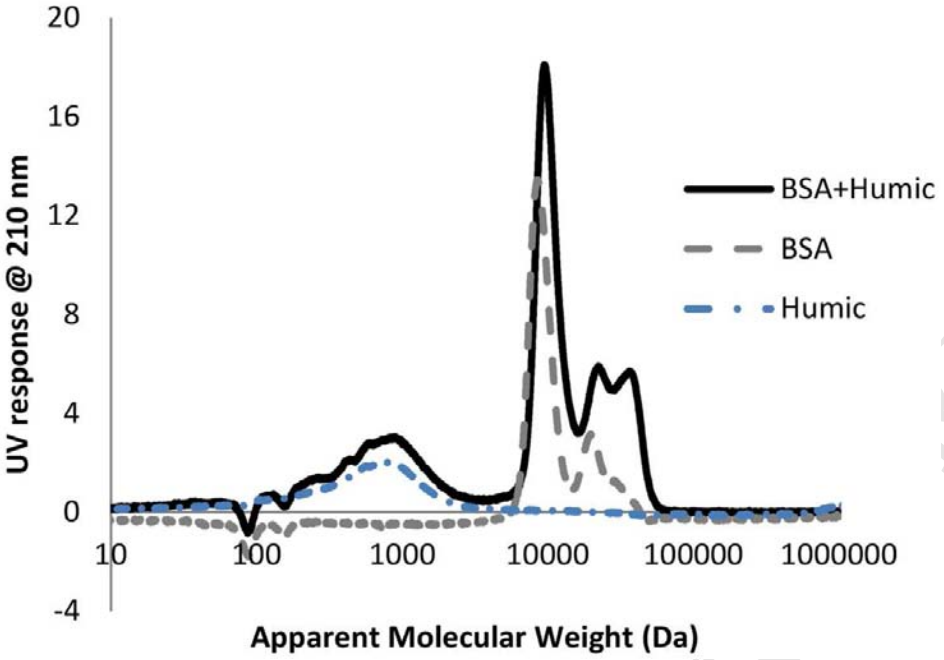

Fig. 9 Chromatograms of UV response at a) 254 nm and b) 210 nm for BSA- humic acid solution in electrolyte (Method A).

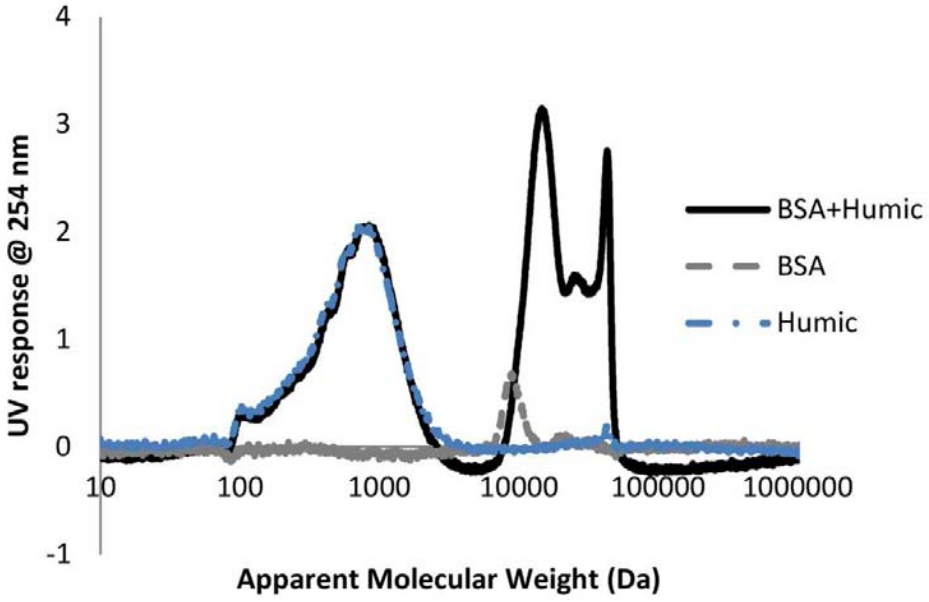

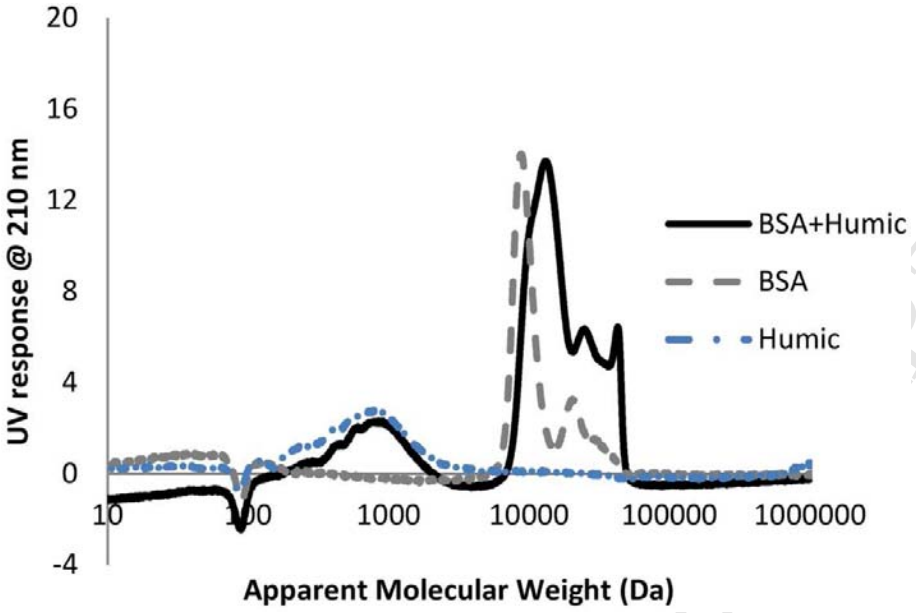

Fig.10 Chromatograms of UV response at a) 254 nm and b) 210 nm for BSA- humic acid solution in water (Method A).

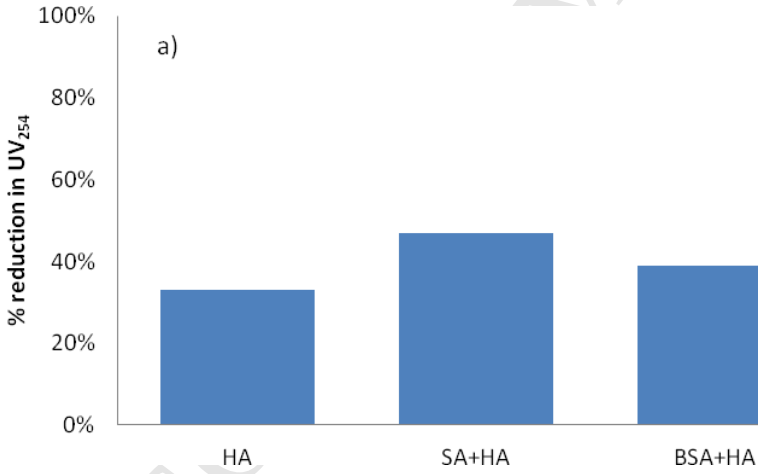

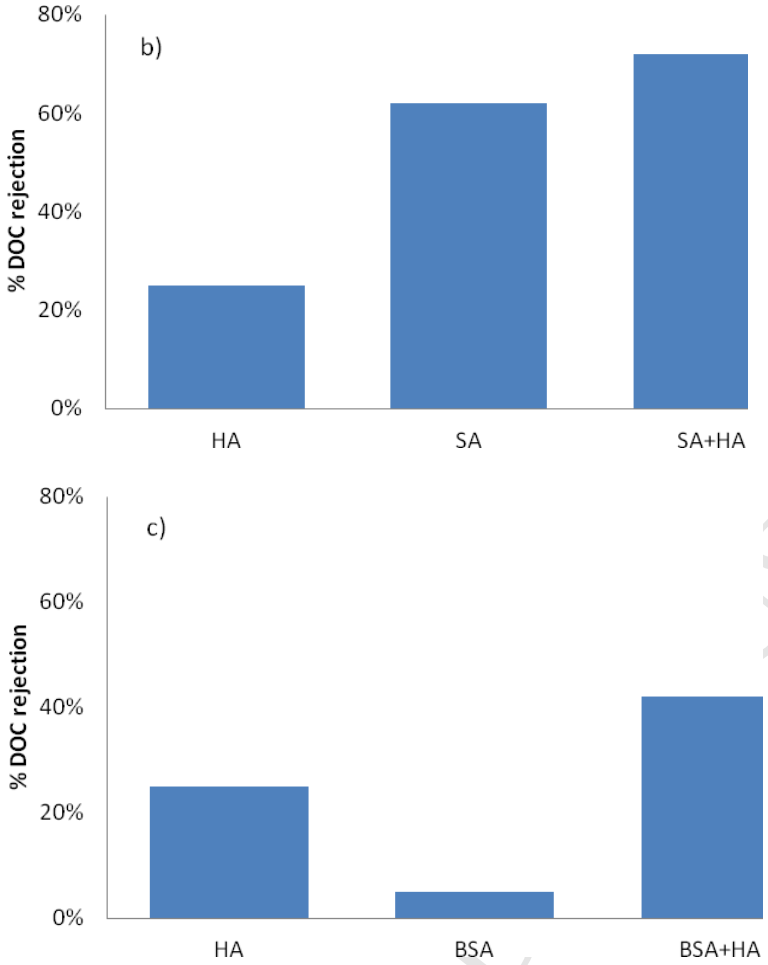

Fig.11 a) % reduction in UV_{254} absorbance in permeate; % rejection in DOC concentration in permeate for b) humic acid (HA), sodium alginate and sodium alginate-humic solutions and c) humic acid (HA), bovine serum albumin (BSA) and BSA-humic solutions

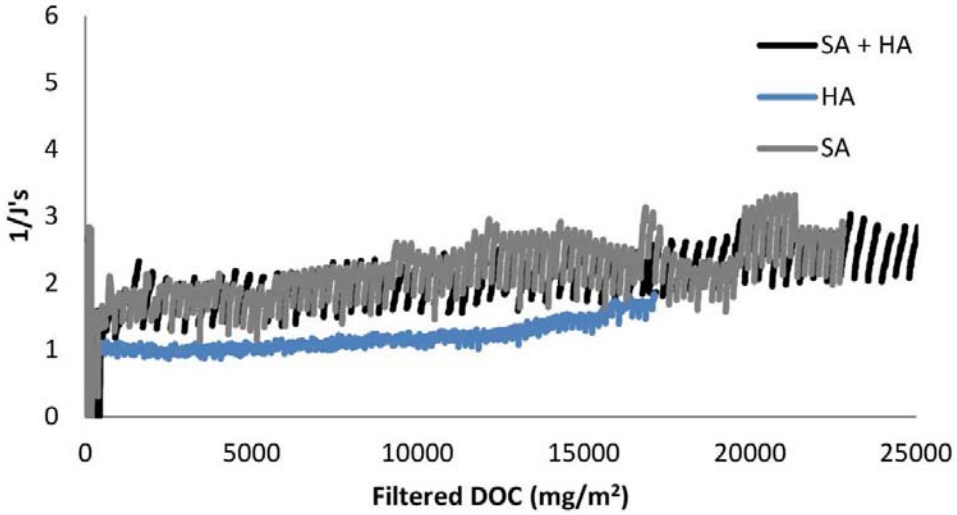

Fig.12 Plot of fouling curves of sodium alginate, humic acid and sodium alginate-humic acid mixture solutions

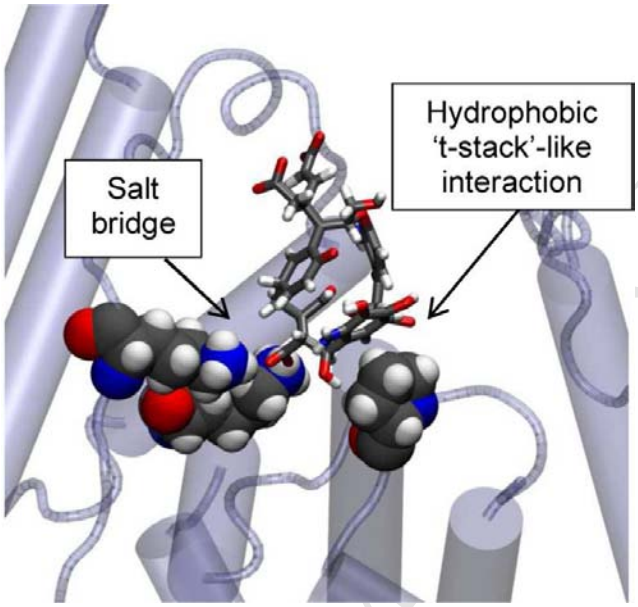

Fig.13. BSA (protein)-humic acid (TNB) attractive interaction, captured in a molecular dynamics simulation. The interacting amino acid residues have been displayed as van der Waals spheres and the TNB model is displayed as tubular (N – blue; O – red, C –black; H – white). A salt bridge interaction may be observed between two $-NH_3^+$ moieties and a deprotonated carboxylate moiety of the humic acid. A hydrophobic 't-stacking'-type interaction may be also observed between the aromatic ring of the humic acid and the aliphatic ring of a proline residue.

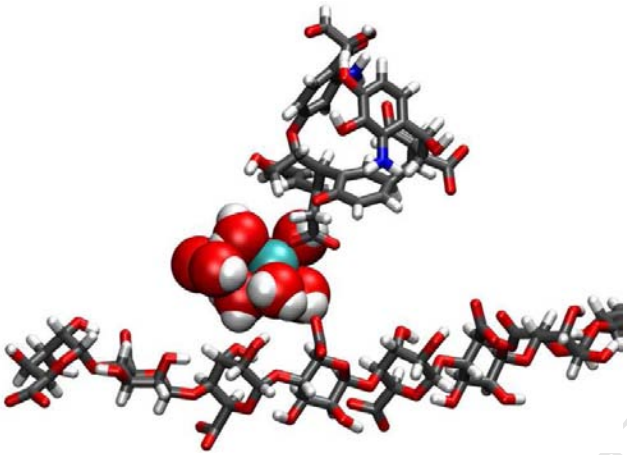

Fig.14. Alginate – humic acid (TNB) attractive interaction, captured during a molecular dynamics simulation. The humic acid molecule (top) and alginate chain (below) is displayed as tubular (N – blue; O – red, C –black; H – white). The Ca^{2+} ion (green) and water molecules are rendered as van der Waals spheres. A direct bond between the carboxylate group of the TNB molecule and a hydrated Ca^{2+} ion can be clearly seen. The interaction between the Ca^{2+} ion and alginate is water-bridged via three hydrogen bonds.